Journal of Oceanology and Limnology
Vol. 36 No. 5, P. 1870-1879, 2018
https://doi.org/10.1007/s00343-018-7228-0

Comparison of otolith shape descriptors and morphometrics for stock discrimination of yellow croaker along the Chinese coast*

SONG Junjie (宋骏杰)[1, 3], ZHAO Bo (赵博)[1, 3], LIU Jinhu (刘金虎)[1], CAO Liang (曹亮)[1], DOU Shuozeng (窦硕增)[1, 2, 3, **]

[1] *CAS Key Laboratory of Marine Ecology and Environmental Sciences*, *Institute of Oceanology*, *Chinese Academy of Sciences*, *Qingdao 266071*, *China*

[2] *Laboratory for Marine Ecology and Environmental Science*, *Qingdao National Laboratory for Marine Science and Technology*, *Qingdao 266071*, *China*

[3] *University of Chinese Academy of Sciences*, *Beijing 100049*, *China*

Received Jul. 31, 2017; accepted in principle Sep. 6, 2017; accepted for publication Oct. 9, 2017

Abstract This study compared and evaluated the efficiency of two otolith shape descriptors (i.e., the elliptic Fourier transform (EFT) and discrete wavelet transform (DWT)) and morphometrics for stock discrimination. To accomplish this, sample fish from three stocks of yellow croaker *Larimichthys polyactis* along the Chinese coast (LDB stock from the Liaodong Bay of the Bohai Sea, JZB stock from the Jiaozhou Bay of the Yellow Sea and CJE stock from the Changjiang River estuary of the East China Sea) were used for otolith morphology analyses. The results showed that morphometrics produced an overall classification success rate of 70.8% in contrast with success rates of 80.0% or 82.0% obtained using EFT or DWT, respectively. This suggests that the two shape descriptors comparably discriminated among the stocks and performed more efficiently than morphometrics. During data adjustment and acquisition, some size variables were excluded from the subsequent discriminant analysis for stock discrimination because they were statistically "ineffective," which could reduce the efficiency of morphometrics and lead to relatively low overall classification success. Both EFT and DWT retain the contour coefficients and thus provide a detailed description of otolith shape, which could improve discriminatory efficiency compared with morphometrics.

Keyword: otolith; stock discrimination; discrete wavelet transform; elliptic Fourier transform; morphometrics; *Larimichthys polyactis*

1 INTRODUCTION

Understanding stock structure is fundamental to fisheries management, and various methods are currently used to delineate the structure of fish stocks based on the analysis of factors such as fish morphology, biology, parasitology, otolith morphology, microchemistry and genetics. Among them, otolith morphology is commonly employed for stock discrimination due to its unique advantages including convenience, low cost and relatively high efficiency (Begg and Waldman, 1999). Otoliths are calcareous crystals in the inner ears of teleosts, and their formation as extracellular depositions is controlled by different biological factors (e.g., growth, metamorphosis and genetics) and environmental conditions (e.g., temperature, habitat and food supply) (Lombarte and Lleonart, 1993; Cardinale et al., 2004). Genetic and environmental factors have interactive effects on otoliths, resulting in variation among geographical stocks that makes otolith morphology a useful tool for stock discrimination (Vignon and Morat, 2010).

* Supported by the National Key Basic Research Program of China (973 Program) (No. 2015CB453302), the NSFC-Shandong Joint Fund for Marine Science Research Centre (No. U1606404), and the Aoshan Science and Technology Innovation Project (No. 2015ASKJ02-04)
** Corresponding author: szdou@qdio.ac.cn

Otolith morphology is generally delineated based on morphometrics and shape descriptors. The morphometrics mainly include the weight, area, perimeter, length, width, angle and several derivative parameters of the otoliths. The shape descriptors are conventionally extracted and analyzed via Fourier transform (FT) techniques, especially elliptic Fourier transform (EFT). The applications of FT in otolith shape analysis can be traced to the 1980s (Bird et al., 1986), but the conventional FT is limited to shapes that have only one intersection between the radius and the outline. Since the 1990s, EFT has been used in otolith shape analysis (Murta et al., 1996), and it has unique advantages over other methods (Crampton, 1995). For example, it does not require equally spaced data points or an explicit definition of a biologically homologous or mathematically determined outline centroid, and EFT can also be applied to a complex curve, independent of the position of the outline on the digitization grid. However, EFT can only be used to analyze the frequency content of a signal, which means that it cannot locate the feature regions of the otolith shape (Libungan and Pálsson, 2015). Additionally, the shape information is allocated to all the Fourier harmonics, which could limit its application to broken otoliths.

Discrete wavelet transform (DWT) is an alternative signal processing method that is defined as the dilations and translations of a basis function. DWT has an infinite set of possible basis functions, so one can develop optimum wavelets for specific analyses (Graps, 1995). Furthermore, DWT is a multi-scale analytical method that analyzes both the time and frequency content of a signal and employs "scale" instead of the conventional "frequency" (Zhang et al., 2013). The method is designed so that high frequency signal components are better resolved in terms of their location, while low frequency values are better estimated but not localized as effectively (Watkinson and Gillis, 2005). If the signal has a discontinuity, only its correlated coefficients would be influenced. All these aspects make DWT sensitive to small differences in otolith shape, and it can also locate the feature regions (Renán et al., 2011). Therefore, DWT has recently been adopted in otolith shape analyses for both species (Parisi-Baradad et al., 2005, 2010; Sadighzadeh et al., 2012) and stock identification (Renán et al., 2011; Eggers et al., 2014; Sadighzadeh et al., 2014; Libungan et al., 2015), and previous studies have suggested that it could effectively extract otolith shape information for stock discrimination.

In recent years, researchers tend to use shape descriptors more often than morphometrics because the reliability and efficiency of morphometrics have been questioned as a delineator for stock discrimination. This is mainly because otolith morphometrics are closely correlated to fish ontogeny, and the routinely practiced size adjustment methods may not be able to reduce the fish effects as effectively as expected. However, few studies have attempted to investigate and compare the efficiency of the two shape descriptors and morphometrics as stock delineators.

The yellow croaker, *Larimichthys polyactis*, is an important demersal sciaenid fish that is widely distributed in Chinese coastal waters from the Bohai Sea southwards to the East China Sea. It generally spawns from April to June in the coastal waters and forages nearby, and then migrates and lives in deeper waters in winter (Ye, 1991). However, due to overfishing in recent decades, yellow croaker populations have dramatically decreased. In addition, the biological traits and ecological features of the species have been markedly affected: simplification of its population structure, earlier maturation and an increasing growth rate (Jin, 1996). For example, the catch of the yellow croaker fishery is now dominated by young-of-the-year, and the size and age of the spawners at first maturation have been decreasing in recent decades. Based on traditional morphometric and meristic characteristics, it has generally been believed that there are three major yellow croaker populations along the Chinese coast: the Bohai Sea-Yellow Sea population, the south Yellow Sea population and the East China Sea population (Ye, 1991). Several studies suggest that environmental changes and increased fishing pressure in recent decades might have affected the habitats, migration and distribution patterns of these fish, thus promoting the occurrence of new stocks or subpopulations (Han et al., 2009; Lin et al., 2008, 2011; Zhang et al., 2016).

Liaodong Bay (LDB), which lies in the northernmost area of the China Sea, has a relatively long ice period, and the large influx of water from several rivers (e.g., the Liaohe River) also affects its hydrology (Li et al., 2010). Jiaozhou Bay (JZB) is a semi-closed bay with limited seawater exchange with the Yellow Sea, and its aquatic environment has been markedly affected by human activities (e.g., large-scale reclamation, aquaculture and industrial sewage discharge) during the past decades (Sun and Sun, 2011). The Changjiang River estuary (CJE) is the estuary of the longest river in China, and the extensive flux of sand and mud from

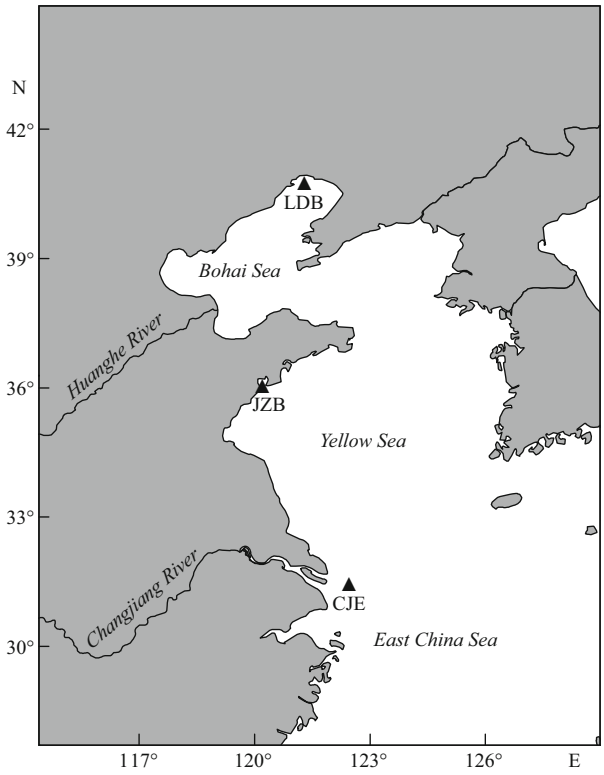

Fig.1 Yellow croaker sampling sites

LDB: Liaodong Bay; JZB: Jiaozhou Bay; CJE: Changjiang River estuary.

the river into the estuary contributes to its unique hydrology and biotic environments (Chen, 2006). The biotic and abiotic differences among these areas likely contribute to their distinct niches, so each yellow croaker geographical group may have different life history traits, stock features or otolith morphologies.

In this study, three geographical stocks of yellow croaker along the Chinese coast were discriminated using two otolith shape descriptors (EFT and DWT) and morphometrics. The main goal was to evaluate the application of DWT to otolith morphology for stock discrimination and to compare its efficiency with the other two analytical methods (EFT and morphometrics). In addition, this study could promote a better understanding of the yellow croaker stocks along the Chinese coast.

2 MATERIAL AND METHOD

2.1 Sample collection

Fish were collected in April to June 2005 from Chinese coastal waters during trawling fishery surveys. The sampling sites included LDB of the Bohai Sea, JZB of the Yellow Sea and CJE of the East China Sea, all of which are yellow croaker spawning areas (Fig.1).

Immediately after capture, the fish were labeled and

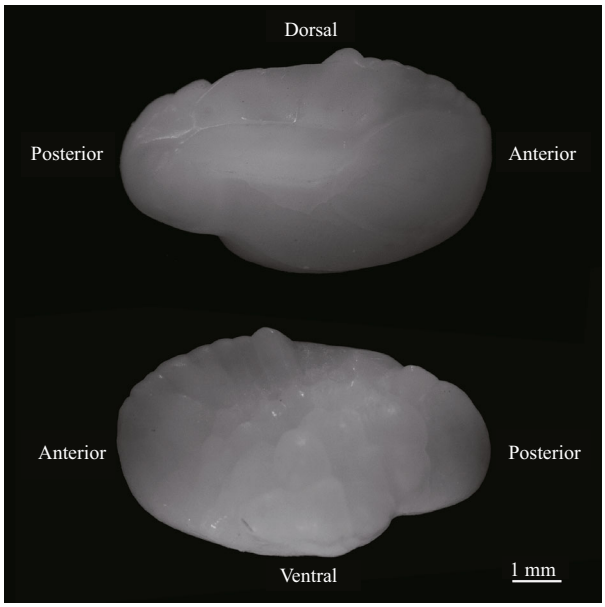

Fig.2 Medial (up) and distal (down) sides of the left otolith of the yellow croaker (144 mm in length)

Table 1 Basic information about the fish samples and otoliths*

Sampling site		CJE	JZB	LDB
Number of sample		65	65	65
Fish length (mm)	Range	135–145	135–145	135–145
	Mean±SD	140.4±3.2	140.0±3.6	139.5±3.2
Otolith weight (mg)	Range	75.82–106.59	68.54–94.50	68.91–89.28
	Mean±SD	90.86±7.15	81.27±6.17	79.66±4.75
Otolith length (mm)	Range	6.97–7.94	6.88–7.58	6.92–7.57
	Mean±SD	7.47±0.22	7.22±0.18	7.19±0.16

* Region codes as in Fig.1.

frozen for subsequent biological analysis. In the laboratory, basic biology was determined and recorded. The sagitta were removed, rinsed with fresh water, air dried and stored in glass vials for subsequent analyses.

In total, 195 specimens (65 from each sampling site) were used in this study, assuming that intra-stock individuals were from the same cohort (Table 1). The Kruskal-Wallis test was adopted to examine the fish length distribution of each sampling site, and no significant differences were observed among sites (P>0.05). Since the otolith morphological parameters of yellow croakers do not significantly differ between sexes or relative to their positions in the body, left otoliths from females were used (Fig.2). Prior to imaging for morphological measurements, the otoliths were rinsed in an ultrasonic cleaner to remove the tissue adhered to the surface, dried in an oven at 35°C, and weighed to the nearest 0.01 mg.

2.2 Data acquisition

For imaging, the medial side (the side with the sulcus) of each otolith was positioned facing up with the anterior side to the right under a binocular microscope (Nikon SMZ1000, Tokyo, Japan) connected to a digital video camera, and ACT-2 software was used to capture the images of the otoliths. The images were then imported into the shapeR package to generate the otolith morphometrics including length, width, area and perimeter. The length and width are the Feret diameters along the major and minor axes, respectively (Libungan and Pálsson, 2015). The shapeR package was also used to generate elliptic Fourier coefficients (EFc) and discrete wavelet coefficients (DWc).

The shapeR package generates 1 024 coordinates on the contour and then transforms them to DWc via Daubechies wavelets. According to Mallat's pyramid algorithm, the number of the finest-scale wavelet coefficients (level 10) is the same as the number of coordinates, i.e., 1 024 (2^{10}), which is then reduced at a rate of 1/2 until the coarsest scale is reached (level 0; only one coefficient; Mallat, 1989). Each elliptic Fourier harmonic has four coefficients, and since EFc normalization is based on the first three coefficients of harmonic 1, these three coefficients are constants and are removed in the subsequent analyses (Kuhl and Giardina, 1982). To determine the number of coefficients adopted, the deviation between the original contour and the reconstruction based on EFc or DWc was calculated (Libungan and Pálsson, 2015), and it was controlled to less than 1% in this study. The first six levels of DWc (63 coefficients) and the first ten Fourier harmonics (37 coefficients) were adopted for the statistical analyses.

2.3 Statistical analysis

To be informative in discriminating among stocks, the variables should be independent of fish size, so the effects of fish length on the parameters (morphometrics, EFc and DWc) were tested by multivariate analysis of covariance (MANCOVA) with sampling site as the factor and fish length as the covariate. The Shapiro-Wilk test and Levene's test were performed to examine data normality and homogeneity of variance, respectively. If any variable did not meet these assumptions, the data were logarithm, square-root, or arcsine transformed. Those variables that did not meet the assumptions even after transformation were excluded from the subsequent analyses, which included one DWc and three EFc in this study. If a significant interaction was detected between sampling site and fish length, the corresponding parameter was excluded from further statistical analyses because it could not be accurately adjusted to remove the length effect (Begg and Brown, 2000); accordingly, two other DWc that showed significant interactions were excluded. The remained parameters that significantly correlated with fish length were adjusted to remove the length effect.

The five morphometric variables (i.e., MPc: length, width, perimeter, area and weight) were adjusted according to the following formula (Lleonart et al., 2000):

$$Y_i^*=Y_i(X_0/X_i)^a,$$

where Y_i^* is the adjusted parameter; Y_i is the original parameter; X_0 is a selected standard fish length (140 mm in this study); X_i is the body length of a specific specimen; and a is the regression coefficient between the logarithmic-transformed parameter and fish length.

The EFc and DWc were adjusted according to the following formula (Cardinale et al., 2004):

$$Y_i^*=Y_i+b(X_0-X_i),$$

where b is the regression coefficient between the parameter and fish length. In both formulae, the regression coefficient is common to all groups.

Since significant collinearity existed among the parameters (MPc, EFc and DWc), principal component analysis (PCA) was performed to generate a new series of orthogonal variables, i.e., principal component scores (PCs). A few PCs could explain most of the variance in the parameters, which reduced the number of variables adopted in the subsequent analyses. In this study, a level explaining 90% of the total variance was set as a criterion to determine the number of PCs. However, since the number of MPc was small (only five), all the PCs were adopted for MPc analysis. When calculating the PCs of the MPc, the correlation matrices were selected. While calculating the PCs of EFc or DWc, the variance-covariance matrices were selected.

The canonical discriminant analysis (CDA) using a stepwise analysis was adopted to evaluate the performance of MPc, EFc and DWc in discriminating among the three yellow croaker stocks. Classification success rates were generated based on leave-one-out cross-validations. In the CDA, homogeneity of the within-group covariance matrices was tested to determine the adoption of a linear (homogenous matrices; using pooled matrix) or quadric (heterogeneous matrices; using within-group

Table 2 Classification success rates for the three yellow croaker groups based on the morphometrics and two shape descriptors*

Parameter	Sampling site	Classification success rate (%)			
		CJE	JZB	LDB	Overall
MPc	CJE	84.6 (55)	15.4 (10)	0	70.8
	JZB	7.7 (5)	64.6 (42)	27.7 (18)	
	LDB	0	36.9 (24)	63.1 (41)	
EFc	CJE	83.1 (54)	6.2 (4)	10.8 (7)	80.0
	JZB	12.3 (8)	83.1 (54)	4.6 (3)	
	LDB	20.0 (13)	6.2 (4)	73.8 (48)	
DWc	CJE	84.6 (55)	4.6 (3)	10.8 (7)	82.0
	JZB	7.7 (5)	83.1 (54)	9.2 (6)	
	LDB	16.9 (11)	4.6 (3)	78.5 (51)	

* The numbers in the parentheses are sample sizes. Region codes as in Fig.1.

matrices) model (Tuset et al., 2003).

To further examine the ability of DWT to discriminate among stocks, mean otolith contours of the yellow croaker stocks were reconstructed using DWc, and the intra-class correlation (ICC) was plotted against the angle to cross-validate the differences in the otolith contours of the stocks (Libungan and Pálsson, 2015).

The statistical analyses were performed in SPSS 20.0 (IBM Corp, Armonk, NY) and SAS 9.4 (SAS Institute, Cary, NC). Differences were considered significant at $P<0.05$.

3 RESULT

The CDA results for stock discrimination among the three sample groups using different otolith morphological parameters are summarized in Table 2 and Fig.3. The correlation coefficients between the discriminant functions and the PCs adopted for stock discrimination, and the main components of each PC are summarized in Appendix Table A1.

3.1 Stock discrimination using MPc

Five MPc were adopted in the PCA, and five PCs were generated, of which four (PC1 to PC4) were used in the CDA. The first canonical discriminant function (F1; eigenvalue, λ=1.922) explained 96.3% of the variance and discriminated the CJE sample from the other two samples well. The F1 was closely correlated to PC1 (correlation coefficient, R=0.912), which explained 72.6% of the variables' variance and was closely correlated to all five MPc. The second canonical discriminant function (F2; λ=0.073)

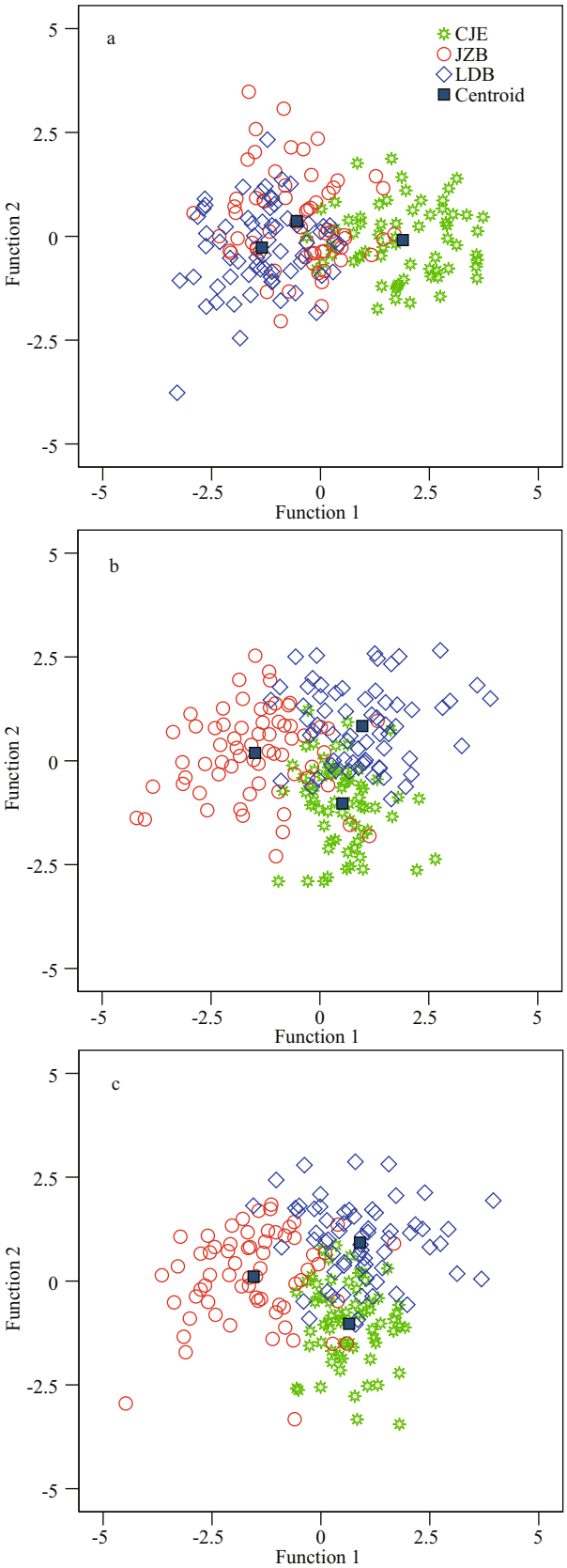

Fig.3 Scatterplots of the two discriminant functions for different morphological parameters

a. MPc; b. EFc; c. DWc.

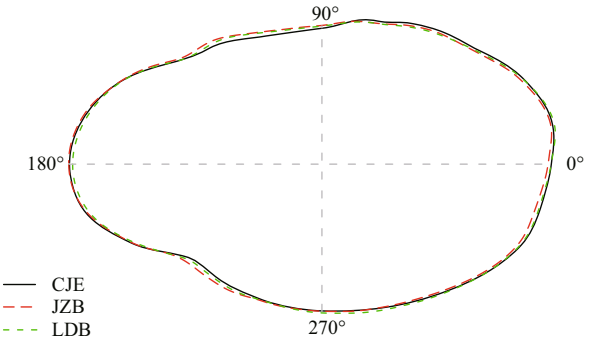

Fig.4 The mean otolith contours of three groups constructed from wavelet coefficients

The numbers along the contours show the angle in degrees (°).

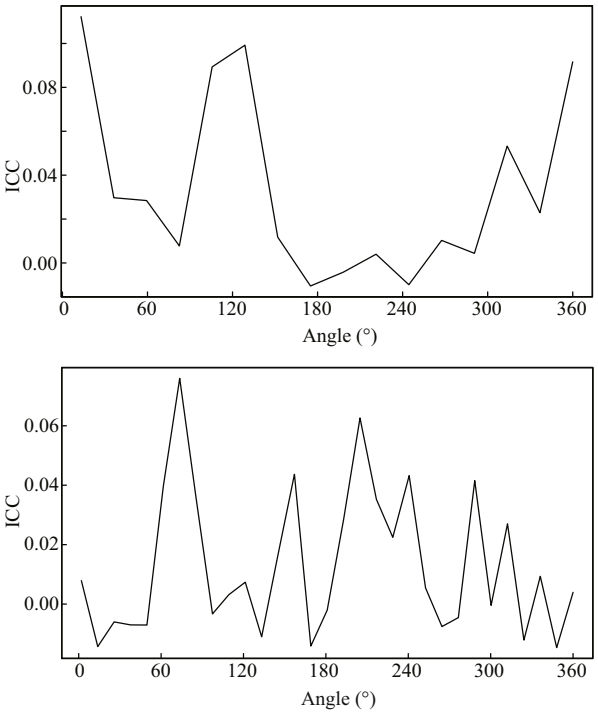

Fig.5 The proportion of variance among groups (ICC) constructed based on level 4 (up) and 5 (down) wavelet coefficients

The horizontal axis shows the angle in degrees (°).

explained 3.7% of the variance and was closely correlated to PC4 (R=0.863), which explained 3.5% of the variables' variance and was relatively more correlated with otolith weight. However, both discriminant functions failed to discriminate between the JZB and LDB samples. The CDA produced an overall classification success rate of 70.8%, with the highest rate for the CJE sample (84.6%), followed by the JZB sample (64.6%) and the LDB sample (63.1%).

3.2 Stock discrimination using EFc

Thirty EFc were adopted in the PCA, and eleven PCs were generated, of which eight (PC1 to PC6, PC9 and PC11) were used in the CDA. The F1 (λ=1.161) explained 65.7% of the variance and discriminated the JZB sample from the other two samples well. The F1 was closely correlated to PC2 (R=0.615) and PC3 (R=-0.529). The F2 (λ=0.606) explained 34.3% of the variance and discriminated between the CJE and LDB samples well. The F2 was closely correlated to PC4 (R=-0.661). The PC2, PC3 and PC4 explained 20.1%, 12.7% and 8.2% of the variables' variance, respectively. These three PCs were mainly correlated with lower EFc. The CDA produced an overall classification success rate of 80.0%, with the highest rate for the CJE (83.1%) and JZB (83.1%) samples, followed by the LDB sample (73.8%).

3.3 Stock discrimination using DWc

Fifty-five DWc were adopted in the PCA, and sixteen PCs were generated, of which nine (PC1 to PC5, PC7, PC9, PC10 and PC14) were used in the CDA. The F1 (λ=1.223) explained 65.2% of the variance and discriminated the JZB sample from the other two samples well. The F1 was closely correlated to PC4 (R=0.615) and PC1 (R=-0.520). The F2 (λ=0.652) explained 34.8% of the variance and discriminated between the CJE and LDB samples well. The F2 was also closely correlated to PC4 (R=0.638) and PC1 (R=0.572). The PC1 and PC4 explained 24.2% and 8.5% of the variables' variance, respectively. These two PCs were mainly correlated with DWc of lower levels. The CDA produced an overall classification success rate of 82.0%, with the highest rate for the CJE sample (84.6%), followed by the JZB sample (83.1%) and the LDB sample (78.5%).

3.4 Mean otolith contours

The mean otolith contours reconstructed based on the DWc are plotted in Fig.4. The otolith contours of the three samples appeared to differ from each other. The ICC plotted against the angle derived from level 4 and 5 DWc showed differences in the otolith contours among the samples (Fig.5). The ICC based on level 4 coefficients had two peaks around 0° and 120°, while the ICC based on level 5 coefficients had several peaks around 80° and 230°. It was obvious that these ICC peaks were consistent with differences in mean otolith contours among the different groups. However, several ICC peaks (around 160° and 300°) based on level 5 coefficients were not consistent with differences in mean otolith contours. Higher levels of DWc (e.g., level 5 in this study) describe contours in

finer detail, but they are more sensitive to the variation among individuals within a stock, which may be one reason for the inconsistency between the ICC and the mean otolith contours.

4 DISCUSSION

Otoliths grow throughout the life of fish, and their external characteristics generally vary among geographic stocks due to differences in their development and environmental history. Therefore, otolith morphology is often used for stock discrimination (Campana and Casselman, 1993; Begg and Brown, 2000; Tuset et al., 2013; Avigliano et al., 2014, 2017). Previous studies have shown that this approach can result in relatively high classification success rates in a variety of fish species. For instance, otolith morphology has been shown to discriminate among stocks at an overall classification success rate of over 80% in Atlantic herring (*Clupea harengus*; Burke et al., 2008), horse mackerel (*Trachurus trachurus*; Stransky et al., 2008), Atlantic saury (*Scomberesox saurus*; Agüera and Brophy, 2011), and sea bass (*Dicentrarchus labra*; Arechavala-Lopez et al., 2012). However, it appears to be less efficient in discriminating among stocks of other fish species, such as Atlantic cod (*Gadus morhua*; Campana and Casselman, 1993), comber (*Serranus cabrilla*; Tuset et al., 2003), roundnose grenadier (*Coryphaenoides rupestris*; Longmore et al., 2010) and tapertail anchovy (*Coilia nasus*; Dou et al., 2012). In the present study, higher overall classification success rate was achieved using the EFT or DWT than using MPc for discriminating among yellow croaker stocks.

The morphometrics (e.g., weight, length, width, perimeter, area or the derivative ratios) of otoliths are usually correlated with each other. Additionally, they are commonly correlated with fish growth and show relatively large individual variations, so data adjustments are routinely performed to remove length effects prior to discriminant analyses. However, many of the size variables are removed during data adjustments, resulting in the exclusion of useful morphological information from the subsequent discriminant analysis. Consequently, only a limited number of size variables are retained for stock discrimination, which may reduce the discriminatory efficiency of morphometrics. This has been clearly demonstrated in previously studied fish such as comber (64%–69%; Tuset et al., 2003), striped trumpeter (*Latris lineata*; 47.2%; Tracey et al., 2006), Atlantic saury (67%; Agüera and Brophy, 2011), mulloway (*Argyrosomus japonicus*; 47.9%; Ferguson et al., 2011) as well as yellow croaker (70.8%; the present study).

Compared to morphometrics, EFc represent otolith contours in detail and extract a finer degree of morphological information from image analysis. Generally, lower-ranking EFc describe the general shape of the otolith, while higher-ranking EFc interpret the detailed shape. Since a large number of EFc from both rankings are retained for stock discrimination in statistical analyses, EFc generally perform more efficiently in discriminating among stocks than morphometrics. For example, in the above-mentioned studies, EFc performed more efficiently than morphometrics, by 26.6%, 25.0% and 9.2% for mulloway (Ferguson et al., 2011), striped trumpeter (Tracey et al., 2006) and yellow croaker (the present study), respectively. In other cases, EFc discriminated among stocks with classification success rates greater than 90% for horse mackerel (Stransky et al., 2008) and three goby species (Lord et al., 2012).

For stock discrimination, Renán et al. (2011) used DWc to analyze otolith shape in groups of red grouper (*Epinephelus morio*) along the northern coast of the Yucatan Peninsula and the Campeche Bank. However, no significant differences in otolith shape were observed among the groups in this study, confirming the lack of stock segregation among the regional groups. Additionally, DWc were used to discriminate between the different snapper (*Lutjanus johnii*) stocks of the Persian Gulf and Oman Sea with modest accuracy (76.2%; Sadighzadeh et al., 2014). For Atlantic herring, otolith shape analyses based on DWc efficiently discriminated between Icelandic and Norwegian spawning stocks with high accuracy (93.6%; Libungan et al., 2015). This approach also allowed for discrimination among the herring stocks in the North Atlantic Ocean (79.2%), similar to the results based on EFc (Libungan and Pálsson, 2015). Moreover, combining DWc with vertebral and growth characteristics was used to successfully confirm the three putative herring stocks along the southern coast of Norway (Eggers et al., 2014). In the present study, both EFc and DWc efficiently discriminated among the three yellow croaker stocks at high classification success rates. These results suggested that DWc efficiently discriminates among stocks at a level comparable to that of EFc. Although both DWc and EFc efficiently represent the fine features of the otolith shape, EFc could not locate the feature regions, which is not a problem when using DWc due to the spatial and frequency localization properties of wavelet

bases (Chuang and Kuo, 1996; Libungan and Pálsson, 2015). Furthermore, the wavelet has different base functions, thus providing specific parameter choices (Graps, 1995; Chuang and Kuo, 1996). In recent years, more studies have used the wavelet in otolith shape analysis (Conroy, 2016; Libungan et al., 2016; Renán et al., 2016). However, the use of these two methods for stock identification remains to be explored on a broader scale, and their specifications are currently under discussion (Stransky, 2014).

As mentioned previously, otolith morphology is usually correlated with fish growth, which is affected by environmental factors such as temperature and other habitat conditions. This has been well demonstrated in the otolith morphometrics of Atlantic cod, which show no significant differences among different stocks under the same temperature and feeding conditions but exhibit significant differences among individuals of the same stock under different growth conditions (Cardinale et al., 2004). For the yellow croaker in the present study, the CJE sample may grow differently than the LDB and JZB samples due to their different environmental histories, particularly the temperatures experienced by the fish (Lin et al., 2011). This could result in the CJE individuals having a unique otolith morphology, discriminating themselves well from the other stocks. However, intra-stock growth variation, even on a small scale, could have significant impacts on the variability in individual otolith morphology, consequently confounding the efficiency of the analyses. Thus, morphological variables are routinely adjusted to remove the length effect (i.e., individual growth variation) of the samples before they are used for discriminant analysis. In the present study, the fish length ranges of the three yellow croaker samples were small, and their distributions were homogeneous. Furthermore, the size adjustment was performed to remove the length effects. All these procedures improved the accuracy of otolith morphology analysis.

It was believed that there are three major yellow croaker populations along the Chinese coast (Ye, 1991). Recent studies suggest that environmental changes and fishing pressure may promote the occurrence of subpopulations (Lin et al., 2008, 2011; Han et al., 2009; Zhang et al., 2016). Nonetheless, the three stocks analyzed in the present study are putatively considered to be discrete geographical stocks. The results of the present study supported this conclusion, indicating that otolith morphology, particularly when using the two shape descriptors, is an efficient and useful tool for discriminating among these stocks.

5 CONCLUSION

In summary, when using otolith morphology to discriminate among yellow croaker stocks, shape descriptors (EFT or DWT) generally resulted in a higher discriminatory efficiency than morphometrics. As a potential method for analyzing otolith morphology that is not yet widely applied, DWT appears to be able to discriminate among stocks as efficiently as EFT.

6 DATA AVAILABILITY STATEMENT

The datasets during and/or analyzed during the current study are available from the corresponding author on reasonable request.

7 ACKNOWLEDGEMENT

We thank the people who contributed to the sample collection and Dr. Yu X for his help with the statistical analysis. We also thank the anonymous reviewers for their constructive comments on the manuscript.

References

Agüera A, Brophy D. 2011. Use of saggital otolith shape analysis to discriminate Northeast Atlantic and Western Mediterranean stocks of Atlantic saury, *Scomberesox saurus saurus* (Walbaum). *Fish. Res*., **110**(3): 465-471.

Arechavala-Lopez P, Sanchez-Jerez P, Bayle-Sempere J T, Sfakianakis D G, Somarakis S. 2012. Discriminating farmed gilthead sea bream *Sparus aurata* and European sea bass *Dicentrarchus labrax* from wild stocks through scales and otoliths. *J. Fish Biol*., **80**(6): 2 159-2 175.

Avigliano E, Domanico A, Sánchez S, Volpedo A V. 2017. Otolith elemental fingerprint and scale and otolith morphometry in *Prochilodus lineatus* provide identification of natal nurseries. *Fish. Res*., **186**: 1-10.

Avigliano E, Martinez C F R, Volpedo A V. 2014. Combined use of otolith microchemistry and morphometry as indicators of the habitat of the silverside (*Odontesthes bonariensis*) in a freshwater-estuarine environment. *Fish. Res*., **149**: 55-60.

Begg G A, Brown R W. 2000. Stock identification of haddock *Melanogrammus aeglefinus* on Georges bank based on otolith shape analysis. *Trans. Am. Fish. Soc*., **129**(4): 935-945.

Begg G A, Waldman J R. 1999. An holistic approach to fish stock identification. *Fish. Res*., **43**(1-3): 35-44.

Bird J L, Eppler D T, Checkley D M Jr. 1986. Comparisons of herring otoliths using Fourier series shape analysis. *Can. J. Fish. Aquat. Sci*., **43**(6): 1 228-1 234.

Burke N, Brophy D, King P A. 2008. Otolith shape analysis: its

application for discriminating between stocks of Irish Sea and Celtic Sea herring (*Clupea harengus*) in the Irish Sea. *ICES J. Mar. Sci*., **65**(9): 1 670-1 675.

Campana S E, Casselman J M. 1993. Stock discrimination using otolith shape analysis. *Can. J. Fish. Aquat. Sci*., **50**(5): 1 062-1 083.

Cardinale M, Doering-Arjes P, Kastowsky M, Mosegaard H. 2004. Effects of sex, stock, and environment on the shape of known-age Atlantic cod (*Gadus morhua*) otoliths. *Can. J. Fish. Aquat. Sci*., **61**(2): 158-167.

Chen J S. 2006. Theories of River Water Quality and Water Quality of Chinese Rivers. Science Press, Beijing. 292p. (in Chinese)

Chuang G C H, Kuo C C J. 1996. Wavelet descriptor of planar curves: theory and applications. *IEEE Trans. Image Process*., **5**(1): 56-70.

Conroy C W. 2016. The behaviors, habitat preferences, and ecology of distinct Atlantic cod phenotypes in the Gulf of Maine. Northeastern University, Boston, Massachusetts. 222p.

Crampton J S. 1995. Elliptic Fourier shape analysis of fossil bivalves: some practical considerations. *Lethaia*, **28**(2): 179-186.

Dou S Z, Yu X, Cao L. 2012. Otolith shape analysis and its application in fish stock discrimination: a case study. *Oceanol. Limnol. Sin*., **43**(4): 702-712. (in Chinese with English abstract)

Eggers F, Slotte A, Libungan L A, Johannessen A, Kvamme C, Moland E, Olsen E M, Nash R D. 2014. Seasonal dynamics of Atlantic herring (*Clupea harengus* L.) populations spawning in the vicinity of marginal habitats. *PLoS One*, **9**(11): e111985.

Ferguson G J, Ward T M, Gillanders B M. 2011. Otolith shape and elemental composition: complementary tools for stock discrimination of mulloway (*Argyrosomus japonicus*) in southern Australia. *Fish. Res*., **110**(1): 75-83.

Graps A. 1995. An introduction to wavelets. *IEEE Comput. Sci. Eng*., **2**(2): 50-61.

Han Z Q, Lin L S, Shui B N, Gao T X. 2009. Genetic diversity of small yellow croaker *Larimichthys polyactis* revealed by AFLP markers. *Afr. J. Agric. Res*., **4**(7): 605-610.

Jin X S. 1996. Ecology and population dynamics of small yellow croaker (*Pseudosciaena polyactis* Bleeker) in the Yellow Sea. *J. Fish. Sci. China*, **3**(1): 32-46. (in Chinese with English abstract)

Kuhl F P, Giardina C R. 1982. Elliptic Fourier features of a closed contour. *Comput. Graph. Image Process*., **18**(3): 236-258.

Li X Z, Liu L S, Li B Q. 2010. Macrobenthos in China Sea: Research and Practice. Ocean Press, Beijing. 378p. (in Chinese)

Libungan L A, Óskarsson G J, Slotte A, Jacobsen J A, Pálsson S. 2015. Otolith shape: a population marker for Atlantic herring *Clupea harengus*. *J. Fish Biol*., **86**(4): 1 377-1 395.

Libungan L A, Pálsson S. 2015. ShapeR: an R package to study otolith shape variation among fish populations. *PLoS One*, **10**(3): e0121102.

Libungan L A, Slotte A, Otis E O, Pálsson S. 2016. Otolith variation in Pacific herring (*Clupea pallasii*) reflects mitogenomic variation rather than the subspecies classification. *Polar Biol*., **39**(9): 1 571-1 579.

Lin L S, Cheng J H, Jiang Y Z, Yuan X W, Li J S, Gao T X. 2008. Spatial distribution and environmental characteristics of the spawning grounds of small yellow croaker in the southern Yellow Sea and the East China Sea. *Acta Ecologica Sinica*, **28**(8): 3 485-3 494. (in Chinese with English abstract)

Lin L S, Liu Z L, Jiang Y Z, Huang W, Gao T X. 2011. Current status of small yellow croaker resources in the southern Yellow Sea and the East China Sea. *Chin. J. Oceanol. Limnol*., **29**(3): 547-555.

Lleonart J, Salat J, Torres G J. 2000. Removing allometric effects of body size in morphological analysis. *J. Theor. Biol*., **205**(1): 85-93.

Lombarte A, Lleonart J. 1993. Otolith size changes related with body growth, habitat depth and temperature. *Environ. Biol. Fishes*, **37**(3): 297-306.

Longmore C, Fogarty K, Neat F, Brophy D, Trueman C, Milton A, Mariani S. 2010. A comparison of otolith microchemistry and otolith shape analysis for the study of spatial variation in a deep-sea teleost, *Coryphaenoides rupestris*. *Environ. Biol. Fishes*, **89**(3-4): 591-605.

Lord C, Morat F, Lecomte-Finiger R, Keith P. 2012. Otolith shape analysis for three *Sicyopterus* (Teleostei: Gobioidei: Sicydiinae) species from New Caledonia and Vanuatu. *Environ. Biol. Fishes*, **93**(2): 209-222.

Mallat S G. 1989. A theory for multiresolution signal decomposition: the wavelet representation. *IEEE Trans. Pattern Anal. Mach. Intell*., **11**(7): 674-693.

Murta A G, Borges M F, Silveiro M L. 1996. Morphological variations in the sagitta otoliths of horse mackerel (*Trachurus trachurus*) in Portuguese waters (Div. IXa). ICES CM 1996/H: 27. 8p.

Parisi-Baradad V, Lombarte A, Garcia-Ladona E, Cabestany J, Piera J, Chic O. 2005. Otolith shape contour analysis using affine transformation invariant wavelet transforms and curvature scale space representation. *Mar. Freshw. Res*., **56**(5): 795-804.

Parisi-Baradad V, Manjabacas A, Lombarte A, Olivella R, Chic Ò, Piera J, García-Ladona E. 2010. Automated Taxon Identification of Teleost fishes using an otolith online database-AFORO. *Fish. Res*., **105**(1): 13-20.

Renán X, Montero-Muñoz J, Garza-Pérez J R, Brulé T. 2016. Age and stock analysis using otolith shape in gags from the southern Gulf of Mexico. *Trans. Am. Fish. Soc*., **145**(6): 1 252-1 265.

Renán X, Pérez-Díaz E, Colás-Marrufo T, Garza-Pérez J R, Brulé T. 2011. Using otolith shape analysis to identify different stocks of *Epinephelus morio* from the Campeche Bank. *In*: Proceedings of the 63rd Gulf and Caribbean Fisheries Institute. San Juan, Puerto Rico. p.200-206.

Sadighzadeh Z, Tuset V M, Valinassab T, Dadpour M R,

Lombarte A. 2012. Comparison of different otolith shape descriptors and morphometrics for the identification of closely related species of *Lutjanus* spp. from the Persian Gulf. *Mar. Biol. Res.*, **8**(9): 802-814.

Sadighzadeh Z, Valinassab T, Vosugi G, Motallebi A A, Fatemi M R, Lombarte A, Tuset V M. 2014. Use of otolith shape for stock identification of John's snapper, *Lutjanus johnii* (Pisces: Lutjanidae), from the Persian Gulf and the Oman Sea. *Fish. Res.*, **155**: 59-63.

Stransky C, Murta A G, Schlickeisen J, Zimmermann C. 2008. Otolith shape analysis as a tool for stock separation of horse mackerel (*Trachurus trachurus*) in the Northeast Atlantic and Mediterranean. *Fish. Res.*, **89**(2): 159-166.

Stransky C. 2014. Morphometric outlines. *In*: Cadrin S X, Kerr L A, Mariani S eds. Stock Identification Methods: Applications in Fishery Science. 2nd edn. Academic Press, New York. p.129-140.

Sun S, Sun X X. 2011. Atlas of Long-Term Changes in the Jiaozhou Bay Ecosystem. Ocean Press, Beijing. 809p. (in Chinese)

Tracey S R, Lyle J M, Duhamel G. 2006. Application of elliptical Fourier analysis of otolith form as a tool for stock identification. *Fish. Res.*, **77**(2): 138-147.

Tuset V M, Lozano I J, González J A, Pertusa J F, García-Díaz M M. 2003. Shape indices to identify regional differences in otolith morphology of comber, *Serranus cabrilla* (L., 1758). *J. Appl. Ichthyol.*, **19**(2): 88-93.

Tuset V M, Parisi-Baradad V, Lombarte A. 2013. Application of otolith mass and shape for discriminating scabbardfishes *Aphanopus* spp. in the north-eastern Atlantic Ocean. *J. Fish. Biol.*, **82**(5): 1 746-1 752.

Vignon M, Morat F. 2010. Environmental and genetic determinant of otolith shape revealed by a non-indigenous tropical fish. *Mar. Ecol. Prog. Ser.*, **411**: 231-241.

Watkinson D A, Gillis D M. 2005. Stock discrimination of Lake Winnipeg walleye based on Fourier and wavelet description of scale outline signals. *Fish. Res.*, **72**(2): 193-203.

Ye C C. 1991. Small yellow croaker (*Larimichthys polyactis*). *In*: Deng J Y ed. Marine Fisheries Biology. China Agriculture Press, Beijing. (in Chinese)

Zhang C, Jiang Y Q, Ye Z J, Li Z G, Dou S Z. 2016. A morphometric investigation of the small yellow croaker (*Larimichthys polyactis* Bleeker, 1877): evidence for subpopulations on the Chinese coast. *J. Appl. Ichthyol.*, **32**(1): 67-74.

Zhang Y D, Wang S H, Ji G L, Dong Z C. 2013. An MR brain images classifier system via particle swarm optimization and kernel support vector machine. *Sci. World J.*, **2013**: Article ID 130134.

Appendix Table A1 Correlation coefficients between the discriminant functions and the PCs adopted for stock discrimination and the main components of each PC

Parameter	PCs	Explained variance	Coefficient		Main components of each PC
			Function 1	Function 2	
MPc	PC1	72.6%	0.912	-0.243	Area (0.971), length (-0.881), weight (-0.875), width (0.815), perimeter (0.696)
	PC2	13.9%	-0.277	-0.024	Perimeter (0.657), weight (0.335), width (-0.330)
	PC3	9.0%	-0.284	-0.443	Width (0.452), length (0.389)
	PC4	3.5%	0.103	0.863	Weight (0.319)
EFc	PC1	24.8%	0.292	-0.406	EFc1d (0.926), EFc3d (-0.440), EFc2d (0.410), EFc4b (-0.366) EFc2b (-0.352)
	PC2	20.1%	0.615	0.416	EFc2b (-0.825), EFc2c (0.748), EFc4b (-0.417), EFc4c (0.400), EFc1d (-0.276)
	PC3	12.7%	-0.529	0.248	EFc2d (-0.739), EFc2c (0.506), EFc10a (0.420), EFc9d (-0.356), EFc3d (0.353)
	PC4	8.2%	-0.003	-0.661	EFc4d (-0.485), EFc3b (0.448), EFc5c (-0.448), EFc4a (-0.416), EFc3c (0.412)
	PC5	7.5%	0.443	0.090	EFc4b (0.421), EFc6c (-0.415), EFc4c (-0.404), EFc3a (-0.387), EFc5a (-0.369)
	PC6	4.5%	0.014	0.251	EFc3c (-0.581), EFc3b (-0.472), EFc7d (0.465), EFc5a (0.436), EFc7c (0.376)
	PC9	2.5%	-0.114	0.290	EFc5d (0.589), EFc7c (-0.562), EFc3a (0.494), EFc6b (0.411), EFc8c (-0.378)
	PC11	1.6%	0.217	-0.085	EFc6c (-0.447), EFc5a (0.425), EFc6d (0.352), EFc4b (0.337), EFc10c (0.274)
DWc	PC1	24.2%	-0.520	0.572	DW1c1 (0.720), DW2c4 (0.586), DW3c1 (-0.566), DW2c1 (0.520), DW1c2 (0.511)
	PC2	14.6%	0.275	-0.005	DW1c2 (-0.620), DW3c8 (0.547), DW1c1 (0.515), DW2c3 (0.441), DW2c1 (-0.420)
	PC3	11.5%	0.248	-0.319	DW2c3 (0.552), DW1c2 (0.528), DW3c5 (-0.484), DW3c4 (0.397), DW3c3 (-0.332)
	PC4	8.5%	0.615	0.638	DW3c4 (-0.512), DW2c3 (-0.501), DW2c4 (0.392), DW3c5 (0.331), DW3c3 (0.305)
	PC5	5.9%	0.183	0.156	DW4c2 (0.594), DW2c1 (0.429), DW2c4 (-0.416), DW3c2 (-0.377), DW5c3 (-0.356)
	PC7	4.3%	0.306	0.148	DW2c1 (0.490), DW3c8 (0.481), DW4c14 (0.287), DW3c2 (-0.278), DW3c5 (-0.210)
	PC9	2.7%	0.182	-0.288	DW4c12 (0.453), DW4c10 (0.395), DW3c6 (0.372), DW3c8 (0.355), DW3c5 (0.336)
	PC10	2.1%	-0.195	0.073	DW4c8 (-0.529), DW4c9 (0.459), DW4c2 (0.448), DW4c7 (0.432), DW4c1 (-0.377)
	PC14	1.2%	0.125	-0.172	DW3c2 (0.422), DW4c3 (-0.306), DW3c3 (0.302), DW4c15 (0.283), DW5c4 (0.282)